

## Biotechnology and Food Sciences

Research article

# Experimental and theoretical investigation of drotaverine binding to bovine serum albumin

Krystian Gałęcki<sup>1</sup>, Gastón Courtade<sup>2</sup>, Aisling McFall<sup>3</sup>,  
Renata Prieschl Teixeira<sup>4</sup>, Maja Grgic<sup>5</sup>, Marta Esteve-Sisteré<sup>6</sup>,  
Rikke Maglemose Westphalen<sup>7</sup>, Agnieszka Kowalska-Baron<sup>1\*</sup>

<sup>1</sup> Institute of General Food Chemistry, Lodz University of Technology, 90-924 Lodz, Poland

<sup>2</sup> Norwegian University of Science and Technology, 7491 Trondheim, Norway

<sup>3</sup> Queen's University Belfast, BT7 1NN, Northern Ireland

<sup>4</sup> Universidade Federal de São Paulo, 04021-001, São Paulo, Brazil

<sup>5</sup> Josip Juraj Strossmayer University of Osijek, 31000, Osijek, Croatia

<sup>6</sup> ETSEA-University of Lleida, 25198 Lleida, Spain

<sup>7</sup> Technical University of Denmark, 2800 KongensLyngby, Denmark

\*agnieszka.kowalska-baron@p.lodz.pl

**Abstract:** *This study was motivated by the need to provide more insight into the possible mechanism of the intermolecular interactions between antispasmodic drug drotaverine and one of the serum albumins (BSA), with the aim to indicate the most probable sites of these interactions. For this purpose both experimental (spectrofluorometric titration at various temperatures) and theoretical (molecular mechanics) methods have been applied. The obtained results clearly showed that drotaverine quenched BSA fluorescence, and the most probable mechanism is static quenching. The negative value of the theoretically predicted binding free Gibbs energy (-23.8 kJ/mol) confirmed the existence of the intermolecular interactions involving drotaverine and one tryptophan within BSA protein and was well agreed with the experimentally determined value of -25.2 kJ/mol.*

**Keywords:** *bovine serum albumin, drotaverine, fluorescence quenching, phosphorescence, molecular docking.*

## Introduction

Due to their extraordinary binding properties, serum albumins are the main transporters of various small molecules including metabolites, waste products, toxins and many drugs. The binding affinity for serum albumins is one of the most important factors affecting the distribution and the active concentration of many administered drugs. Ligands bound to these transporters are distributed through the circulatory system to their place of function or disposal with no threat of precipitation or undesirable effects [1].

Serum albumins are highly abundant transport proteins present in the blood plasma of mammals [2]. Their structure is composed of  $\alpha$ -helices organized in three similar domains (I-III) each of which is further grouped into two subdomains (A and B), with six and four helices, respectively [3]. The evolution of serum albumins led them to contain several binding sites, allowing them to bind a variety of compounds [4] including two drug sites (Drug Site I and II) [1] which are responsible for interactions with the ligands of a dual lipophilic/anionic character. Drug site 1 is a pre-formed binding pocket within the core of subdomain IIA that comprises all six helices of the subdomain and a loop-helix feature contributed by subdomain IB. The interior of the pocket is predominantly apolar with two clusters of polar residues, the inner cluster towards the bottom of the pocket and the outer one at the pocket entrance. Drug site 2, 1 is topologically similar to site 1 since it is composed of all six helices of subdomain IIIA and comprises a pre-formed hydrophobic cavity with distinct polar features. In terms of shape, size and polarity, the two drug sites in Human Serum Albumin (HSA) are clearly distinguishable, which helps to account for the different binding specificities of the two pockets [1]. Previously reported structural data [1] showed that the two primary drug sites on HSA are highly adaptable binding cavities containing distinct sub-compartments, and reveal a range of secondary binding sites located widely across the protein. The shape and the particular distribution of basic and polar residues on the mainly hydrophobic interior walls that are involved in specific interactions with small ligands determine the binding specificities of the pockets.

Although serum albumins domains exhibit extensive structural homology (Bovine Serum Albumin (BSA) and HSA have over 70% sequence identity and almost 90% sequence similarity [3]), they differ in the distribution of their binding sites. The principal regions of ligand binding to HSA and BSA are located in hydrophobic cavities in subdomains IIA and IIIA.

HSA has one tryptophan (Trp214) located in the subdomain IIA (inside the DS1 cavity), while BSA has two tryptophanyl residues (Trp213 and Trp134). The location of Trp213 is the same as Trp214 (in HSA), while Trp134 is inside the cavity of subdomain IB [5,6]. Due to the presence of tryptophanyl residue(s) in serum albumins, it is possible to apply spectroscopic methods to study ligand binding to these proteins.

Drotaverine 1-(3,4-diethoxybenzilidene)-6,7-diethoxy-1,2,3,4-tetrahydroisoquinoline) is an antispasmodic drug used in the treatment of smooth muscle spasm. It is a selective phosphodiesterase IV inhibitor preventing the hydrolysis of cyclic AMP leading to smooth muscle relaxation. It acts directly on smooth muscle and therefore has no anticholinergic effects reducing the number of side effects. It is used in treating renal colic and has also been used to accelerate labor, but not reduce pain [7,8]. In the structure of drotaverine, shown in Figure 1, the presence of a tetrahydroisoquinoline ring and phenyl group may be noticed

which provide a high level of conjugation and  $\pi$  electrons, thus enabling its detection by UV-Vis and fluorescence spectroscopy.

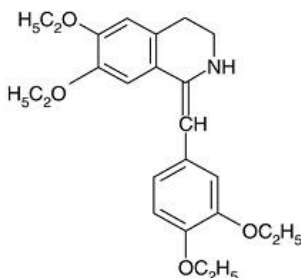


**Figure 1.** The structure of drotaverine

In this study the intermolecular interactions between drotaverine and BSA were investigated with the aim to provide more insight into the possible mechanism of binding of this drug to serum albumins and to its pharmacokinetics. For this purpose both spectroscopic (steady state and time resolved fluorescence) and molecular modeling tools (AutoDock 4.2) were used which allowed to estimate the thermodynamic parameters characterizing binding of this drug to serum albumin and also to indicate the possible location of the binding sites.

## Experimental

### Materials

BSA, drotaverine, potassium iodide (KI), sodium sulfite ( $\text{Na}_2\text{SO}_3$ ) purchased from Sigma-Aldrich were of the highest purity grade and were used without further purification. Stock solutions of phosphate buffer (1 M),  $\text{Na}_2\text{SO}_3$  (0.1 M) and KI (1 M) were freshly prepared using high-purity water (18.2 M $\Omega$ ) from Milli-Q system. Stock solution of BSA (10  $\mu\text{M}$ ) was prepared using 0.05 M phosphate buffer (pH 7). Since the solubility of drotaverine in water is very low, the stock solution of this drug (1 mM) was prepared using 2-propanol.

### Methods

Absorption measurements were made using a Nicolet Evolution 300 UV-Vis spectrophotometer from Thermo Electron Corporation using Vision Pro program. Measurements were carried out within the range of 200-400 nm, with scan speed 120 nm/min and bandwidth 1.5 nm.

Steady-state fluorescence measurements were performed with a FluoroMax4 (JobinYvonSpex) spectrofluorometer, using excitation wavelengths of 295 nm and 370 nm for BSA and drotaverine, respectively. All measurements were performed in a standard quartz cuvette at 20°C.

Fluorescence lifetime measurements were carried out at 20°C with a FL900CDT time-correlated single photon counting fluorometer from Edinburgh Analytical Instruments. The excitation and emission wavelengths were set to 295 nm and 350 nm, respectively. Data acquisition and analysis were performed using the software provided by Edinburgh Analytical Instrumentation.

Fluorometric titrations of drotaverine quenching of BSA fluorescence were carried out at various temperatures (22°C, 26°C, 32°C, 37°C and 42°C) using 10 µM BSA and drotaverine ranging from 0-13 µM. The excitation and emission wavelengths were set to 280 nm and 360 nm, respectively.

Phosphorescence measurements were made on a homemade system. A general description of the equipment for phosphorescence measurements has previously been given [9]. Since molecular oxygen is known to be a strong quenching agent, it was efficiently removed from the sample before the phosphorescence measurements. O<sub>2</sub> removal was achieved by the application of moderate vacuum and inlet of ultrapure nitrogen. The pre-purified nitrogen gas (0.1 ppm of O<sub>2</sub>) was further purified by passing through an oxygen-trapping filter. This degassing procedure was additionally accompanied by the addition of 0.3 ml of 0.1 M Na<sub>2</sub>SO<sub>3</sub> as an O<sub>2</sub> scavenger (final concentration of Na<sub>2</sub>SO<sub>3</sub> in the sample was 0.01 M). Additionally, the presence of Na<sub>2</sub>SO<sub>3</sub> stabilized the iodide solution and prevented the formation of iodine. The sample (BSA solution (20 µM) with 0.01 M Na<sub>2</sub>SO<sub>3</sub>) was placed in a quartz cuvette, which was connected to the N<sub>2</sub>/vacuum line by tubing. Five cycles of deoxygenation were performed. After deoxygenation, the cuvette was moved into the phosphorimeter, but remained attached to the tubing and was allowed to equilibrate to 30°C before taking measurements. The background emission was determined by measurements carried out before deoxygenation of the sample and was subtracted from the phosphorescence decay. All phosphorescence decays, after subtraction of the background, were analyzed in terms of a sum of exponential components by a nonlinear least squares fitting algorithm using the software provided by Origin Pro 8.0.

The binding conformation of BSA and drotaverine was predicted using the Autodock 4.2 software package [10-12] which uses an empirical free energy force field with a Lamarckian Genetic Algorithm to predict the binding conformation and the free energies of association [10]. The structures of BSA and drotaverine were downloaded from the RCSB protein databank [13] and the Drugbank database [7], respectively. Before running the docking simulation the BSA file was prepared using the H++ server [14] to protonate the BSA molecule to replicate its structure at pH 6.5. During the docking analysis the grid size was set to 50, 58, and 48 along X-, Y-, and Z-axis with 0.414 Å grid spacing. The following AutoDocking parameters were used: GA population size = 150; maximum number of energy evaluations = 2500000; GA crossover mode = 2 points. The lowest binding energy conformer was searched out of ten different

conformers for each docking simulation. PyMOL software was also used to visualize the docking conformations.

## Results and Discussion

### Photophysical parameters of BSA and drotaverine

In agreement with previous studies [15,16], the absorption spectrum of BSA in phosphate buffer showed the maximum at 278 nm with the molar absorption coefficient equal to  $(3.38 \pm 0.08) \cdot 10^4 \text{ cm}^{-1} \text{ M}^{-1}$  [17]. The emission spectra of BSA in phosphate buffer showed the broad maximum located at about 345 nm, which is consistent with the previously reported literature data [18].

Also, the fluorescence quantum yield of BSA determined using the comparative method of Williams et al. [19] in which tryptophan with known quantum yield value of 0.14 [20] was applied as a standard sample, was consistent with the previously reported value of 0.19 [17].

In the absorption spectrum of aqueous drotaverine, three maxima, located at 242 nm, 303 nm, and 355 nm, may be noticed, in the agreement with the previously reported values for drotaverine hydrochloride in water [21,22]. The determined molar absorption coefficients were found to be  $(1.86 \pm 0.13) \cdot 10^4 \text{ cm}^{-1} \text{ M}^{-1}$ ,  $(9.64 \pm 0.70) \cdot 10^3 \text{ cm}^{-1} \text{ M}^{-1}$  and  $(1.03 \pm 0.07) \cdot 10^4 \text{ cm}^{-1} \text{ M}^{-1}$  at 242, 303 and 355 nm, respectively.

The emission spectrum of aqueous drotaverine showed a structured band with the maximum located at 456 nm and a shoulder at 425 nm. Previously reported fluorescence spectrum of drotaverineHCl in 0.1 M  $\text{H}_2\text{SO}_4$  showed the maximum located at 465 nm (after excitation at 295 nm) [23].

### Time resolved fluorescence experiments

The decay curves of BSA fluorescence upon increasing concentration of drotaverine were obtained by use of excitation at 295 nm and emission at 350 nm. The fluorescence data (fluorescence lifetimes ( $\tau_1$ ,  $\tau_2$ ) with their fractional contribution ( $f_1$ ,  $f_2$ ) to the steady state intensity), determined from a biexponential fit to time-resolved data, are presented in Table 1. The average lifetime of BSA ( $\tau_{av}$ ) was calculated from  $\tau_{av} = \sum_{i=0}^n \tau_i f_i$  [24]. The goodness of fit was judged from the reduced  $\chi^2$  values.

In the absence of drotaverine, the fluorescence decay of BSA was biexponential with the lifetimes of 6.48 ns and 2.33 ns. The shorter lifetime component, most probably, arises from the 134 tryptophanyl residue which is located in the subdomain IB of the protein and is more exposed to solvent (less „buried” inside the protein) as compared to the emitting Trp213 residue located in the subdomain IIA, to which longer lifetime component may be assigned.

Upon increasing concentration of drotaverine, the fluorescence decay of BSA was also biexponential with no considerable changes in the fluorescence lifetime components. Also, the calculated value of the average fluorescence lifetime of

BSA has not been changed significantly with increasing concentration of drotaverine, suggesting the involvement of static quenching mechanism.

**Table 1.** Time-resolved fluorescence data of BSA upon increasing concentration of drotaverine

$C_{\text{drotaverine}}[\mu\text{M}]$	$\tau_1$ [ns]	$f_1$	$\tau_2$ [ns]	$f_2$	$\tau_{\text{av}}$ [ns]	$\chi^2$
0	6.48±0.07	0.95	2.33±0.60	0.05	6.27±0.06	1.11
7	6.38±0.05	0.96	1.51±0.35	0.04	6.20±0.04	1.20
17	6.44±0.08	0.93	2.32±0.40	0.07	6.15±0.06	1.16
20	6.42±0.06	0.94	2.06±0.36	0.06	6.14±0.07	1.13
27	6.38±0.08	0.93	2.22±0.36	0.07	6.11±0.05	1.14

### Steady-state fluorescence quenching studies

Changes in the fluorescence spectrum of BSA (with the maximum located at about 345 nm) upon increasing concentration of drotaverine are shown in Fig. 2. From Fig. 2, a considerable decrease in the fluorescence intensity of BSA may be seen with increasing concentration of drotaverine.

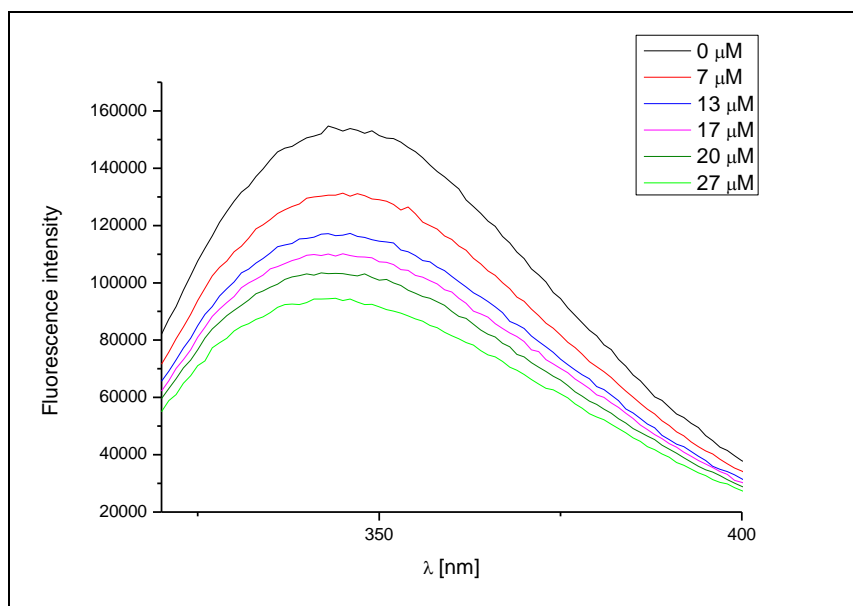


**Figure 2.** Fluorescence spectrum of BSA in phosphate buffer (33  $\mu\text{M}$ ) together with its changes upon increasing concentration of drotaverine

Assuming that static quenching mechanism is involved in the interactions between BSA and drotaverine, the spectrofluorometric titration experiment was performed using very small doses of drotaverine within the concentration range of 0-13  $\mu\text{M}$  at different temperatures. For each temperature, the association

constant ( $K_a$ ) was determined using the Stern-Volmer equation (eq. 1) of the following form:

$$\frac{F_0}{F} = 1 + K_a[Q] \quad (\text{eq. 1})$$

where  $F_0$  and  $F$  are fluorescence intensities of BSA in the absence and presence of the quencher (drotaverine), respectively, and  $[Q]$  is the concentration of the quencher. An example of the Stern-Volmer plot for BSA fluorescence quenching by drotaverine at 22°C is presented in Fig. 3.

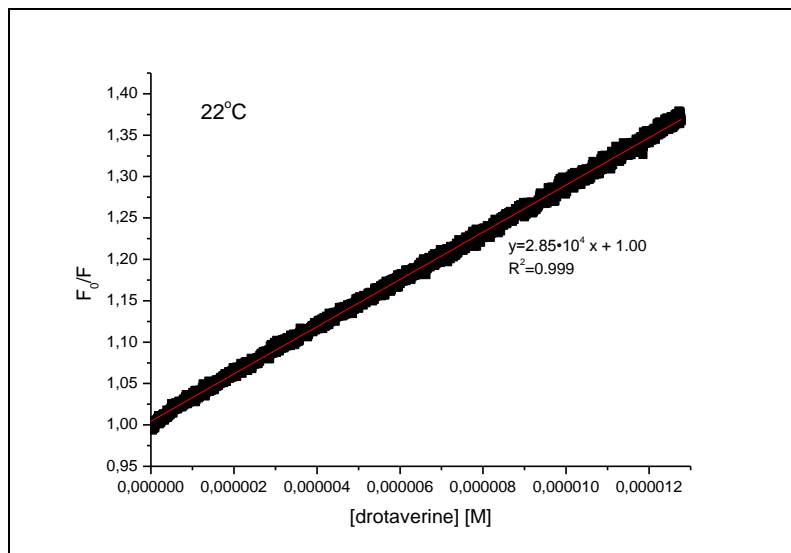


**Figure 3.** Stern-Volmer plot for fluorescence quenching of BSA by drotaverine at 22°C

The determined  $K_a$  values together with their  $R^2$ -values, which are the measure of the goodness of the fit to Stern-Volmer model, are gathered in Table 2. From Table 2 a decrease in  $K_a$  upon increasing temperature may be noticed suggesting involvement of static quenching mechanism between drotaverine and BSA. If the dynamic quenching mechanism prevailed, increasing temperature would lead to an increase in  $K_a$  because of the higher likelihood of collisional quenching [24].

**Table 2.** The determined Stern-Volmer quenching constants ( $K_a$ ) for different temperatures (T)

T [K]	$K_a$ [ $M^{-1}$ ]	$R^2$
295.15	$(2.85 \pm 0.02) \cdot 10^4$	0.999
300.15	$(2.75 \pm 0.01) \cdot 10^4$	0.998
305.15	$(2.57 \pm 0.02) \cdot 10^4$	0.998
310.15	$(2.31 \pm 0.04) \cdot 10^4$	0.994
315.15	$(2.13 \pm 0.03) \cdot 10^4$	0.994

### Thermodynamic parameters characterizing binding of drotaverine to BSA

Considering that binding of drotaverine to BSA is governed mainly by static quenching process, that is, the BSA-drotaverine complex is formed in the ground state, we have calculated (from  $K_a$ -values compiled in Table 2) the thermodynamic parameters for binding of drotaverine to BSA. The thermodynamic parameters such as enthalpy ( $\Delta H$ ), free Gibbs energy ( $\Delta G$ ) and entropy ( $\Delta S$ ) were calculated by following thermodynamic equations:

$$\ln \frac{K_{a2}}{K_{a1}} = \frac{1}{R} \cdot \left( \frac{1}{T_1} - \frac{1}{T_2} \right) \cdot \Delta H \quad (\text{eq.2})$$

$$\Delta G = -R \cdot T \cdot \ln K_a = \Delta H - T \cdot \Delta S \quad (\text{eq. 3})$$

where  $K_a$  is the binding (association) constant at the corresponding temperature and  $R$  is the gas constant. The obtained results are presented in Table 3.

**Table 3.** Thermodynamic parameters for drotaverine binding to BSA

T [K]	$\Delta G$ [kJ/mol]	$\Delta H$ [kJ/mol]	$\Delta S$ [J/(Kmol)]
295.15	-25.17	-5.57	66.40
300.15	-25.51	-10.38	50.41
305.15	-25.76	-16.67	29.79
310.15	-25.91	-12.73	42.47

It is tempting to analyze the obtained thermodynamic parameters in the light of the previously proposed [25] relationship between thermodynamic parameters and binding mode. Ross and Subramanian [25] reported the characteristic signs of the thermodynamic parameters associated with the various individual kinds of interactions that might take place in protein association processes. When  $\Delta H < 0$  or  $\Delta H \approx 0$  and  $\Delta S > 0$  the main acting force is electrostatic interaction [26]. However, it should be kept in mind, that even the electrostatic forces are prevailing in binding drotaverine to BSA, the contributions from hydrophobic, hydrogen bonding, dispersion or van der Waals forces cannot be neglected.

### Phosphorescence measurements

To study the interactions between BSA and drotaverine in the triplet excited state  $T_1$ , the phosphorescence lifetime of BSA was measured upon increasing concentrations of drotaverine at constant concentration of KI, which is a suitable enhancer of intersystem crossing. The obtained results (Fig. 4) showed that the phosphorescence lifetime ( $\tau_{ph}$ ) of BSA increases upon increasing the concentration of drotaverine.



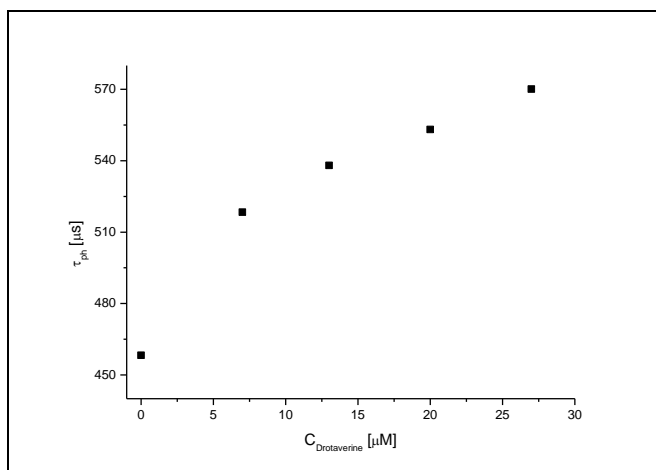


**Figure 4.** Phosphorescence lifetime ( $\tau_{ph}$ ) of BSA vs increasing concentrations of drotaverine

This observation confirms the existence of the intermolecular interactions between drotaverine and BSA in excited triplet state. Most probably, binding drotaverine to BSA triplet state resulted in a considerable stiffening of protein structure in the nearest neighborhood of the emitting tryptophan residue, which is manifested by the observed increase of BSA phosphorescence lifetime upon increasing concentration of drotaverine. This remarkable sensitivity of tryptophan phosphorescence lifetime to the subtle changes associated with binding drugs to tryptophan containing proteins indicate interesting research area in the pharmacokinetic and pharmacodynamics studies.

### Modeling results

A force-field docking simulation of drotaverine to BSA was carried out in AutoDock 4.2 as described in the Materials and Methods section of this paper. The lowest energy configuration of BSA-drotaverine complex, chosen for further analysis, is presented in Fig. 5. The calculated binding free energy for this complex is  $\Delta G = -23.77$  kJ/mol at 298.15 K and correlates well with the value determined from fluorimetric titration experiment. Analyzing the geometrical parameters of the theoretically predicted BSA-drotaverine complex it may be noticed that the lowest energy binding site for drotaverine in BSA was in the vicinity of Trp213.

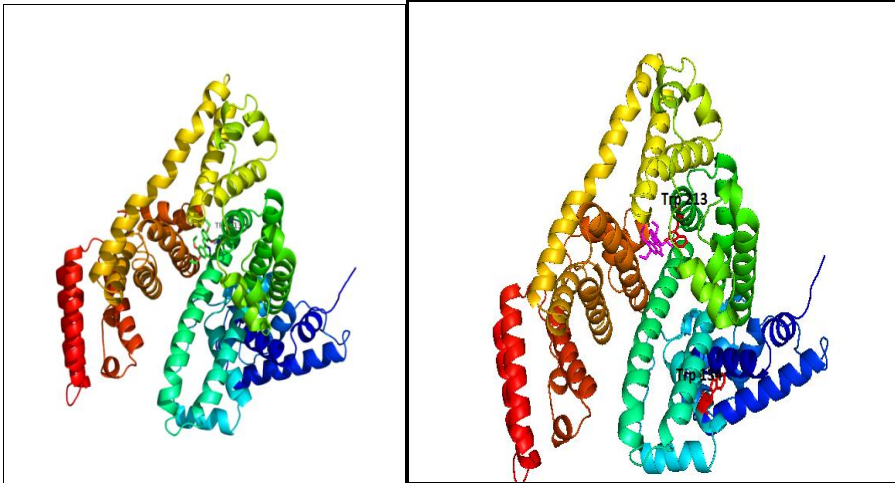


**Figure 5.** Graphical representation of the lowest energy conformation of BSA-drotaverine complex

## Conclusions

The results of this study provided evidence for the existence of intermolecular interactions between drotaverine and BSA. The obtained results clearly showed that drotaverine quenched BSA fluorescence, and the most probable mechanism is static quenching. The experimentally determined free energy of drotaverine binding to BSA was in excellent agreement with the theoretically predicted value estimated from computer simulations. The AutoDock model also revealed that the lowest energy binding site is in drug site I in the vicinity of Trp213. Further research on the topic should include a more detailed study of the interactions in the  $S_1$  and  $T_1$  states. The investigation into the BSA-drotaverine interactions reported here may provide an invaluable structural framework for the interpretation of drug binding data and may facilitate efforts to modify new therapeutic compounds to control their interaction with serum albumins and therefore optimize drug distribution.

## Acknowledgements

The authors would like to thank Prof. S. Wysocki, head of the Institute of General Food Chemistry, who funded the project and provided the equipment. We acknowledge IAESTE for the opportunity to gain invaluable work experience.

## References

1. Ghuman J, Zunszain PA, Petitpas I, Bhattacharya AA, Otagiri M, Curry S. Structural basis of the drug-binding specificity of human serum albumin. *J Mol Biol* **2005**, 353:38-52.
2. Schreiber G, Urban J. The synthesis and secretion of albumin. *Rev Physiol Biochem Pharmacol* **1978**, 82:27-95.

3. Sekula B, Zielinski K, Bujacz A. Crystallographic studies of the complexes of bovine and equine serum albumin with 3,5-diiodosalicylic acid. *Int J Biol Macromol* **2013**, 60:316-324.
4. Doolittle RF. Reconstructing history with amino acid sequences. *Protein Sci* **1992**, 1:191-200.
5. Carter DC, Chang B, Ho JX, Keeling K, Krishnasami Z. Preliminary crystallographic studies of four crystal forms of serum albumin. *Eur J Biochem* **1994**, 226:1049-1052.
6. Peterman BF, Laidler KJ. Study of reactivity of tryptophan residues in serum albumins and lysozyme by N-bromosuccinamide fluorescence quenching. *Arch Biochem Biophys* **1980**, 199:158-164.
7. <http://www.drugbank.ca/drugs/DB06751>
8. Sharma A, Schulman SG. Introduction to fluorescence spectroscopy. John Wiley & Sons, Inc., New York, **1999**, pp. 58-59.
9. Kowalska-Baron A, Chan M, Gałęcki K, Wysocki S. Photophysics of indole, tryptophan and N-acetyl-L-tryptophanamidetryptophan (NATA): heavy atom effect. *Spectrochim Acta A* **2012**, 98:282-289.
10. Morris GM, Huey R, Lindstrom W, Sanner MF, Belew RK, Goodsell DS, Olson AJ. AutoDock4 and AutoDockTools4: Automated docking with selective receptor flexibility. *J Comput Chem* **2009**, 30:2785-2791.
11. Cosconati S, Forli S, Perryman AL, Harris R, Goodsell DS, Olson AJ. Virtual Screening with AutoDock: Theory and practice. *Expert Opin Drug Dis* **2010**, 5:597-607.
12. Forli S, Olson AJ. A force field with discrete displaceable waters and desolvation entropy for hydrated ligand docking. *J Med Chem* **2012**, 55:623-638.
13. <http://www.rcsb.org/pdb/explore/explore.do?structureId=4f5s>
14. Anandakrishnan R, Aguilar B, Onufriev AV. H++ 3.0: automating pK prediction and the preparation of biomolecular structures for atomistic molecular modeling and simulation. *Nucleic Acids Res* **2012**, 40:537-541.
15. Huang P, Kong Y, Li Z, Gao F, Cui D. Copper selenidenanosnakes: bovine serum albumin-assisted room temperature controllable synthesis and characterization. *Nano Lett* **2010**, 5:949-956.
16. Nafisi S, Panahyab A, Sadeghi BB. Interactions between  $\beta$ -carboline alkaloids and bovine serum albumin: investigation by spectroscopic approach. *J Lumin* **2012**, 132:2361-2366.
17. Mishra B, Barik A, Priyadarsini K, Mohan H. Fluorescence spectroscopic studies on binding of a flavonoid antioxidant quercetin to serum albumins. *J Chem Soc* **2005**, 117:641-647.
18. Moriyama Y, Ohta D, Hachiya K, Mitsui Y, Takeda K. Fluorescence behaviour of tryptophan residues of bovine and human serum albumins in ionic surfactant solutions: a comparative study of the two and one tryptophan(s) of bovine and human albumin. *J Protein Chem* **1996**, 15:265-272.
19. Williams ATR, Winfield SA, Miller JN. Relative fluorescence quantum yields using a computer controlled luminescence spectrometer. *Analyst* **1983**, 108:1067-1068.
20. Szabo AG, Rayner DM. Fluorescence decay of tryptophan conformers in aqueous solution. *J Am Chem Soc* **1980**, 101:554-563.
21. Daabees HG. Selective differential spectrophotometric methods for determination of niclosamide and drotaverine hydrochloride. *Anal Lett* **2000**, 33:639-656.

22. Géher J, Szabó É. Computer-aided spectrophotometric determination of multicomponent drugs. *J Pharm Biomed Anal* **1988**, 6:757-764.
23. El-Wasseef DR, El-Sherbiny D, Eid M, Belal F. Spectrofluorometric determination of drotaverine hydrochloride in pharmaceutical preparations. *Anal Lett* **2008**, 41:2354-2362.
24. Lakowicz JR. Principles of fluorescence spectroscopy. Kluwer Academic/Plenum Publishers, New York, **1999**, pp. 129-130.
25. Ross PD, Subramanian S. Thermodynamics of protein association reactions: forces contributing to stability. *Biochemistry* **1981**, 20:3096-3102.
26. Bi S, Yan L, Sun Y, Zhang H. Investigation of ketoprofen binding to human serum albumin by spectral methods. *Spectrochim. Acta A* **2011**, 78:410-414.